ACS APPLIED MATERIALS & INTERFACES

Research Article

www.acsami.org

Ionic Liquid-Assisted Synthesis of Multicolor Luminescent Silica Nanodots and Their Use as Anticounterfeiting Ink

Li Zhou,[†,‡] Andong Zhao,[†,‡] Zhenzhen Wang,[†,‡] Zhaowei Chen,[†,‡] Jinsong Ren,*[,†] and Xiaogang Qu*[,†]

[†]Laboratory of Chemical Biology and State Key Laboratory of Rare Earth Resource Utilization, Changchun Institute of Applied Chemistry, Chinese Academy of Sciences, Changchun, Jilin 130022, China

[‡]Graduate School of the Chinese Academy of Sciences, Beijing 100039, China

Supporting Information

ABSTRACT: Here we propose a simple route for the fabrication of silica nanodots which are strongly photoluminescent in both solution and the solid state based on the use of ionic liquids (ILs). It is found that the ILs not only provides the environment for the reaction but also contributes to the quantum yield (QY) of the silica nanodots. In particular, the produced silica nanodots also displayed excitation-dependent photoluminescence and temperature sensitive properties. Based on the unique optical properties, the as-prepared nanomaterial was used for anticounterfeiting application and the results demonstrated the great potential of the silica nanodots alone or combined with other fluorescent material of unicolor for an improved anticounterfeiting technology. This simple approach and the resulting outstanding combination of properties make the prepared silica nanodots highly promising for myriad applications in areas such as fluorescent anticounterfeiting, optoelectronic devices, medical diagnosis and biological imaging.

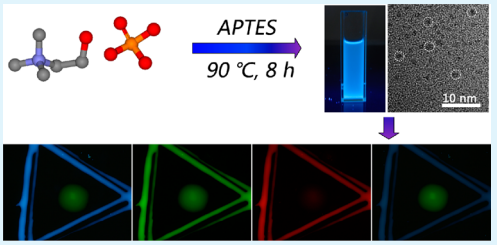

KEYWORDS: *silica, nanodots, ionic liquid, anticounterfeiting, fluorescence*

1. INTRODUCTION

Silicon based functional materials have attracted tremendous attention in the past decades owing to their unique properties and potential applications, including photonics, adsorption, separation, catalysis, and biomedicine material, among others.[1−13] For photonics applications, the key goals has been the development of methods to control the dimensional and surface state of the silicon material since bulk silicon is a spectacularly inefficient light emitter.[2,14] Recent advances in the synthesis of fluorescent silicon nanomaterial allow them to be formed from large-size silicon structures (e.g., silicon nanowires or bulk silicon) by top-down approaches, or from silicon precursors by bottom-up methods.[15−23] Typically, the resulting silicon nanocrystals require further modification to render them stable or water-soluble.[24−28] Alternatively, some one-step reduction strategies have been shown to be efficient in the synthesis of surface-passivated silicon nanoparticle.[29−32] However, it has been suggested that harsh conditions and/or specific equipment are necessary to obtain the nanocrystalline silicon (<5 nm). More recently Hsieh et al. reported the fabrication of quasi-zero dimensional fluorescent silica (SiO_x, silicon oxide) nanodots from hydrolysis of alkylalkoxysilane under an ambient "'air'" atmosphere.[33] Moreover, the use of the silica nanodots as multicolor photoluminescence source for intravital imaging has been demonstrated. While this report has provided a new insight into the fabrication of silicon-based fluorescent nanomaterials, the long alky chains on the surface of the silica nanodots would hinder their use in a wide range of technologies. Herein for the first time we report a simple ionic liquid-assisted one-step method to water-soluble, surface-covered photoluminescent silica nanodots and further extend their application as anticounterfeiting inks.

Ionic liquids (ILs) have been widely studied as a new kind of reaction media due to their high fluidity, low melting temperature and extended temperature range in the liquid state, air and water stability, low toxicity, nonflammability, high ionic conductivity, and importantly no measurable vapor pressure.[34] Significant progress has been made in their applications to biphasic reactions, chemical synthesis, electrochemistry, catalysis, polymerization and biocatalysis.[35−38] In recent years the synthesis of inorganic nano- and microstructures with unique shape and structure in ILs has received increasing attention.[39−46] It has been demonstrated that ILs-based synthetic route not only produces materials with interesting morphologies but also renders them with novel and improved functionalities.[41,47−52] For instance, uniform anatase TiO_2 nanocuboids with extremely high crystalline phase stability had been successfully prepared using ionic liquid as solvent.[47] Micro silica spheres (~50 μm) were also fabricated with rationally selected ILs, which showed an increase in the conducting properties.[49] In contrast to their widely application in organic chemistry, the use of ILs in inorganic synthesis is still in its primary stage. In the current study we report the synthesis of highly photoluminescent silica nanodots with water-dispersity and photostability using choline dihydrogen phosphate (CDP) as additive. Some fascinating features are

Received: November 26, 2014
Accepted: January 12, 2015
Published: January 12, 2015

DOI: 10.1021/am5083304
ACS Appl. Mater. Interfaces 2015, 7, 2905−2911

described in the present work. (i) This method is very simple. The synthesis of ultrasmall silica is a one-step process that does not require high temperature or high pressure apparatus. (ii) The ILs CDP, a green solvent, plays a strategic role on the surface state and thus the quantum yields (QY) of the silica nanodots. The CDP of high concentration could also act as cross-linker for the fluorescent silica nanodot-ILs hybrid gel-like structure with intense fluorescence in both hydrated and dried forms. (iii) The luminescence measurements suggest that the as-synthesized silica nanodots are stable at different pH and ionic strengths, and possess excitation-dependent emission properties. More importantly, we have found that the as-prepared silica nanodots feature a high temperature sensitivity of both their fluorescence intensity and lifetime. Due to the unique luminescence properties, a preliminary investigation of their anticounterfeiting performance has been made. The results indicate that the luminescent color tuning capability, temperature sensitivity and high concealment make these nanoparticles behave in a similar way to chameleons and can provide a strengthened and more reliable anticounterfeiting effect.

2. EXPERIMENTAL SECTION

2.1. Chemicals. Choline hydroxide and phosphoric acid were obtained from Beijing Chemical Reagent Co., Ltd. (China). (3-Aminopropyl) trimethoxysilane (97%) (APTMS) was purchased from Sigma-Aldrich. Ultrapure water (18.2 MΩ; Millpore Co., USA) was used throughout the experiment.

2.2. Synthesis of ILs. The synthesis involved (1:1 mol ratio) neutralization reaction of choline hydroxide and the phosphoric acid. The resulting reaction mixture was evaporated at reduced pressures to obtain crude product. Activated charcoal was then added to the crude compound, stirred with water and filtered. The filtrate was again evaporated to obtain the pure liquid in 98% yield. The product was characterized by electrospray mass spectroscopy and only the expected anion and cation were observed. Electrospray mass s pectroscopy analysis: ES^+, 103.7 ($Me3N^+CH2CH2OH$, 100); ES^-, 96.7 (dihydrogen phosphate, 100).

2.3. Synthesis of silica nanodots. ILs with the designed concentration was first dissolved in water (15 mL) at room temperature. APTMS (5 mL) was added dropwise to the above solution and stirred at 90 °C for 8 h. Subsequently the reaction solution was cooled to room-temperature naturally. The resulting fluorescent product was subjected to dialysis in order to obtain the pure silica nanodots. For the fluorescent silica xerogel, the resulting gel-like structure was frozen at −20 °C for 1 h and then lyophilized for the optical analysis.

For a control experiment, the products were prepared with diluted HCl and sodium dihydrogen phosphate under identical conditions.

2.4. Quantum yield (QY) measurements. The quantum yield (QY) of silica nanodots was measured by comparing the integrated photoluminescence intensities and the absorbency values with the reference quinine sulfate (QS). The QS (literature Q = 0.54) was dissolved in 0.1 M H_2SO_4 and the silica nanodot was dissolved in distilled water. The optical density is kept below 0.05 to avoid inner filter effects. The QYs of the silica nanodots are calculated using following equation:

$$Q = Q_R \frac{I}{I_R} \frac{OD_R}{OD} \frac{n^2}{n_R^2}$$

Where Q is the QY, I is the integrated intensity, OD is the optical density, and n is the refractive index. The subscript R refers to the reference fluorephore of known quantum yield.

2.5. Measurements and characterizations. FT-IR analyze was carried out on a Bruker Vertex 70 FT-IR Spectrometer. SEM images were obtained with a Hitachi S-4800 FE-SEM. UV−vis spectra were recorded with a JASCO-V550 spectrofluorometer. TEM images were recorded using a FEI TECNAI G2 20 high-resolution transmission electron microscope operating at 200 kV. Fluorescence measurements were carried out on a JASCO FP-6500 spectrofluorometer at 25 °C.

3. RESULTS AND DISCUSSION

The silica nanodots were synthesized by hydrolysis of (3-Aminopropyl) trimethoxysilane (APTMS) at 90 °C in the presence of CDP. The atomic force microscopy (AFM) and transmission electron microscopy (TEM) measurements were used for characterization of structure and morphology of the silica nanoparticles, revealing the products appeared as spherical particles with good monodispersity (Figure 1). The size

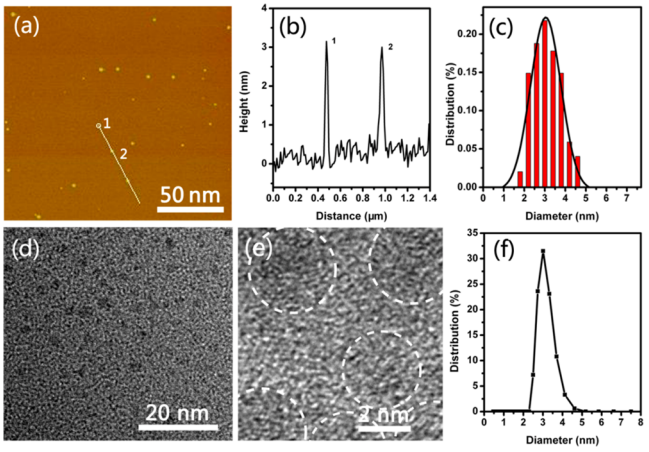

Figure 1. (a) AFM image of silica nanodots on a mica substrate. (b) Height profile along the line in (a). (c) Height distribution of silica nanodots measured by AFM. (d, e) TEM and high resolution TEM images of the silica nanodots. (f) Diameter distribution of silica nanodots measured by DLS.

distribution in Figure 1c calculated by measuring more than 200 particles, showed an average size of 3.0 nm. The diameter measured by dynamic light scattering (DLS) further confirmed the small size of the products with a hydrodynamic diameter of 3.9 nm (Figure 1f). FT-IR spectra of the silica nanodots showed absorption bands at 1570 and 957 cm^{-1} associated with bending vibrations of N−H and stretching vibration of P−O, indicating the existence of amino groups and ILs ligand on the products (Figure 2a). The EDX pattern and XPS spectra revealed that the silica nanodots contained Si, O, N and P elements (Figure 2b, Figure S1), further demonstrating the presence of ILs on the materials. The UV−vis absorption spectrum of the material exhibited a clear adsorption feature at ca. 270 and 305 nm, suggesting the production of silica nanodots as neither the ILs nor APTMS displayed typical absorption at these regions (Figure S2). When excited at 350 nm, the product displayed strong blue PL centered at approximately 445 nm, with a QY determined to be 20.04% (Table S1).

DOI: 10.1021/am5083304
ACS Appl. Mater. Interfaces 2015, 7, 2905−2911

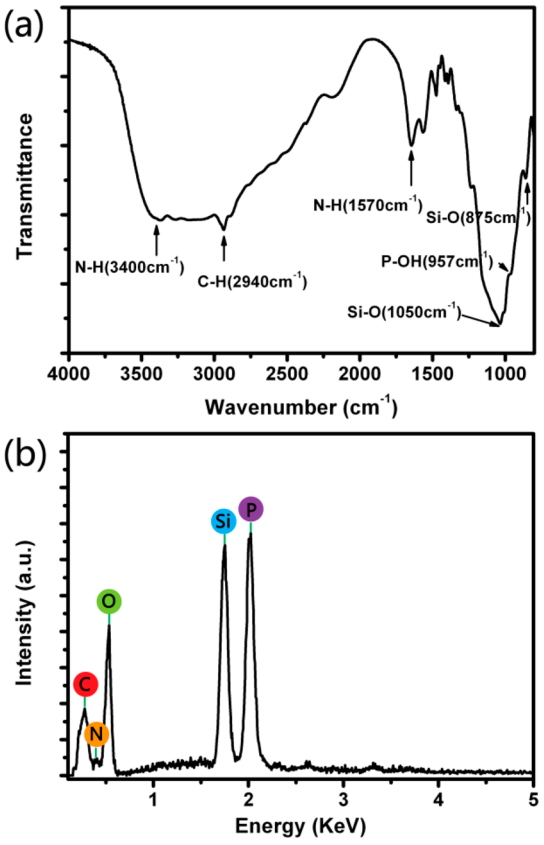

Figure 2. FT-IR spectrum (a) and EDS spectrum (b) of the material prepared with ILs.

Reaction parameters were investigated, including the reaction temperature, time and ILs concentration. Clear solutions with weak PL were observed at room temperature and at 50 °C whereas highly luminescent product formed in the case of 90 °C (Figure S3), suggesting that temperature accelerated the rate of reaction and played an essential role in the formation of the luminescent silica nanodots. At 90 °C, the PL intensity of the products increased over a time range of 2−8 h (Figure S4), which might be ascribed to the gradual hydrolysis of precursor molecules. When the initial ILs concentration was increased from 0 to 1.8 M, the QY of the obtained products increased from 1.5% to 20. 04% (Figure 3a, Table S1), indicating that ILs played a role on the material synthesis. We proceeded to investigate the exact role that the ILs played for the resulting luminescent materials. The acidic environment of the ILs was first probed by performing experiment in the presence of aqueous solution with pH adjusted in accordance with ILs by HCl (0.01 M). From the spectra, it appeared that the pH of the ILs influenced the production of the materials and the QY of the product was determined to be 9.64% (Figure S5, Table S1). Based on the QY of the solution with ILs (20.04%), it was clear that CDP-based ILs, through a combination of charged dihydrogen phosphate anionic group and choline cationic group, could not only provide the acid environment for hydrolysis but also contribute to the QY of the products. It was likely that the anionic dihydrogen phosphate group, bounded to the amino group of −Si−O-Si- network and facilitated clustering by hydrogen bridging, which was in accordance with the previous reports.[6] The choline group may also bound to the dihydrogen phosphate group and, through it, to the −Si−O-C−O-Si network. In this respect, we propose that the

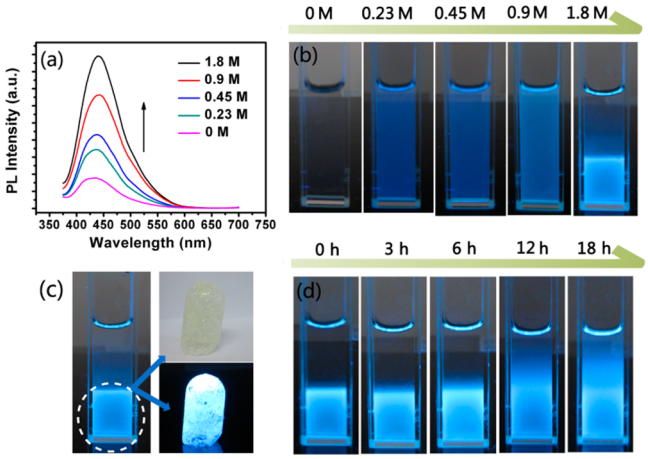

Figure 3. (a, b) PL spectra (λ_{ex} = 350 nm) and photograph of silica nanodots solution (under 365 nm irradiation) prepared with increasing concentration of ILs. (c) Photograph of dried silica gel under daylight (up) and UV irradiation (bottom). (d) Photograph of silica gel dispersed in aqueous solution with increasing time.

emitting states originate from the introduction of defect in the silica network, which was in accordance with the previous reports.[4,6] In addition, gel-like product was obtained when the concentration of ILs reached 1.8 M (Figure 3b). To investigate the role that the CDP played during the process, the material was first prepared in the presence of dihydrogen phosphate solution of the same pH. As shown in Figure S6, the dihydrogen phosphate displayed similar effects but a lower QY (15.1%) as compared to the CDP. To further explore this result, choline chloride solution of the same pH was used to carry out the same experiment. In striking contrast, the product produced was weakly luminescent solution with QY of 10.41% (Table S1), which further confirmed that the dihydrogen phosphate played a major role in the synthesis. Previous report has shown that CDP could be used as biocompatible cross-linking agents for various types of biomaterials through hydrogen bonding.[53] Based on the observation that gel-like product could only be obtained when the concentration of CDP reached 1.8 M, it was likely that the CDP (dihydrogen phosphate) functionalized on the surface of silica nanodots and in the aqueous solution could act as cross-linking agents to get the gel-like product. In addition, the dried product also exhibited bright PL under UV-light excitation (Figure 3c), which was beneficial for photonics and luminescent displays. The stability of the silica gel was further assessed. The gel retained its stability for two months when kept in ILs solution and the dried silica gel was also stable for more than two months at room temperature (Figure S7, Figure S8). However, the luminescent gel-like structure was gradually dissolved when placed in water (Figure 3d), which could be ascribed to the diffusion of the cross-linker (CDP) to the upper aqueous solution.

Next, the optical properties of silica nanodots were investigated. Figure 4a and 4b showed the PL of the material were generally broad and dependent on excitation wavelengths, which as in their silicon counterparts may reflect not only effects from particles of different sizes in the sample but also a distribution of different emissive sites on each protected silica nanodot. The PL of the silica nanodots was stable with respect to photoirradiation, exhibiting no meaningful reduction in the observed intensities in the experiment of continuously

DOI: 10.1021/am5083304
ACS Appl. Mater. Interfaces 2015, 7, 2905−2911

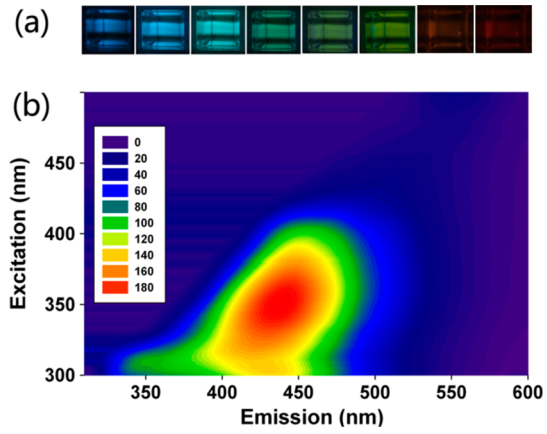

Figure 4. (a) Photograph of silica nanodots solution excited from 350 to 560 nm. (b) 2D excitation−emission topographical maps of silica nanodots.

repeating excitations for several hours (Figure 5a). Further studies showed that there were no changes in PL intensity at

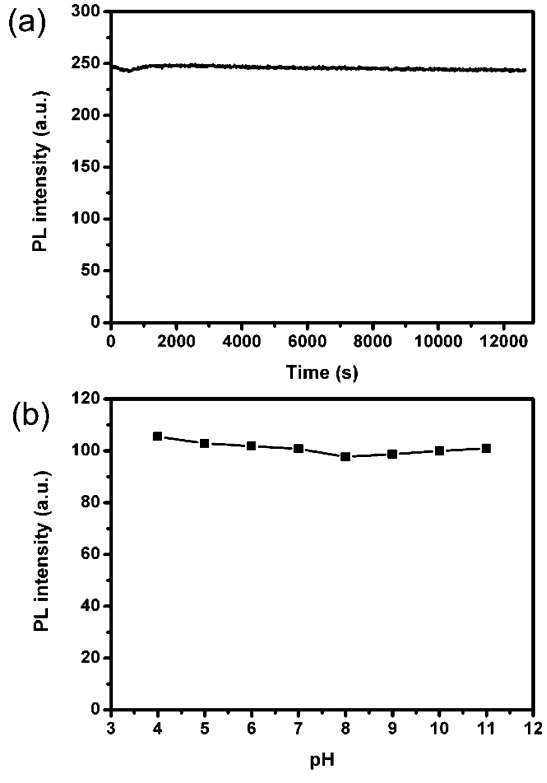

Figure 5. PL intensity of silica nanodot with(a) increasing UV irradiation time and (b) dispersed in PBS under various pH values.

different pH (Figure 5b), which was significant for silica nanodots to be used in the practical applications. The PL lifetime (τ) of the silica nanodots was assessed by time-resolved PL measurements. As seen in Figure S9, the decay curves of the products fitted well to triple-exponential and an average lifetime was calculated to be 9.01 ± 0.05 ns, which was comparable to reported values.[30]

We further searched the effect of temperature on the PL of the silica nanodots. Figure S10 in the Supporting Information displayed pronounced temperature dependence of the fluorescence emission spectra of the silica nanodots solution, with the PL decreasing upon increasing the temperature. Different from QDs that displayed remarkable temperature-dependent spectral shifts, the emission spectra of silica nanodots did not shift within the investigated temperature window. The PL intensity of the silica nanodots film also decreased upon increasing the temperature, revealing similar temperature-dependent PL properties with the solution when excited at 360 nm (Figure 6a, Figure S11 in the Supporting Information).

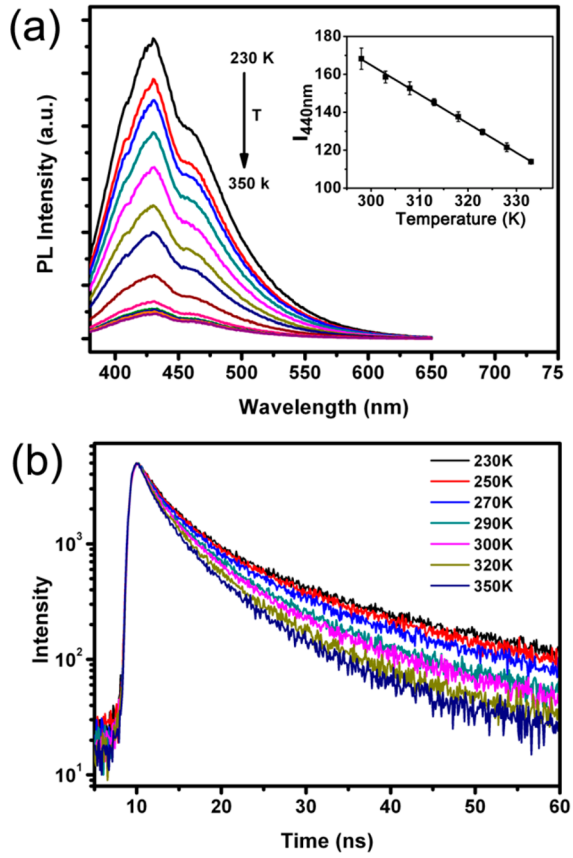

Figure 6. (a) PL spectra of a silica nanodots solution and film at various temperatures. (b) PL decays curve of an interval silica nanodots film at various temperatures. Inset to a: PL intensity of silica nanodots versus temperature and the corresponding linear fit (line).

The PL wavelengths of the films were slightly different from those of the silica nanodots solutions, which was most likely because of energy transfer among the inhomogeneously distributed emitting species in the solid film. The linearity and inverse relationship between the temperature and the PL intensity was evident in an Arrhenius plot (see Figure S10 in the Supporting Information and Figure 6a, inset), which revealed the constant thermal sensitivity of the silica nanodots. Concomitant with the intensity decrease, the fluorescence decay of the silica nanodots accelerated with increasing temperature (Figure 6b). The main contribution to the thermal response of silica nanodots may be attributed to the dominating role of nonradiative recombination.[8] Figure S12 in the Supporting Information showed that the temperature-dependent quenching processes was reversible, suggesting the great potential for using our silica nanodots in the fabrication of temperature-sensitive devices.

During the past decades, anticounterfeiting has attracted much attention because of the widespread forgery in all kinds of

DOI: 10.1021/am5083304
ACS Appl. Mater. Interfaces 2015, 7, 2905−2911

paper documents, package, or certificates. Many technologies against counterfeiting or for detection of forgery have been developed.[54−56] Among them, fluorescent anticounterfeiting technologies have received significant attention and have become indispensable in this field by virtue of their high concealment properties. Currently, intensive research has been concentrated on exploring novel fluorescent nanomaterials with unique properties that are too difficult for counterfeiters to replicate.[57−61] Herein by taking advantage of the excitation-dependent and temperature-sensitive fluorescence, we explored the potential of the as-prepared silica nanodots for improving anticounterfeiting effect (see Figure S13 in the Supporting Information). Counterfeiting of stamps which are specific to certain departments is a very widely used artifice by counterfeiters. Thus, a stamp carved with a pattern on the surface was first prepared to explore whether the silica nanodots could be used in field of anticounterfeiting stamps by the excitation-dependent luminescence. The stamp was dipped in the dispersion of silica nanodots and then stamped on transparent glass substrates. As shown in Figure S8 in the Supporting Information, no obvious pattern could be observed from the transparent glass in daylight. When part of the stamped region was exposed to UV, blue, and green light, clear strokes with multiple colors were observed (Figure 7a). These

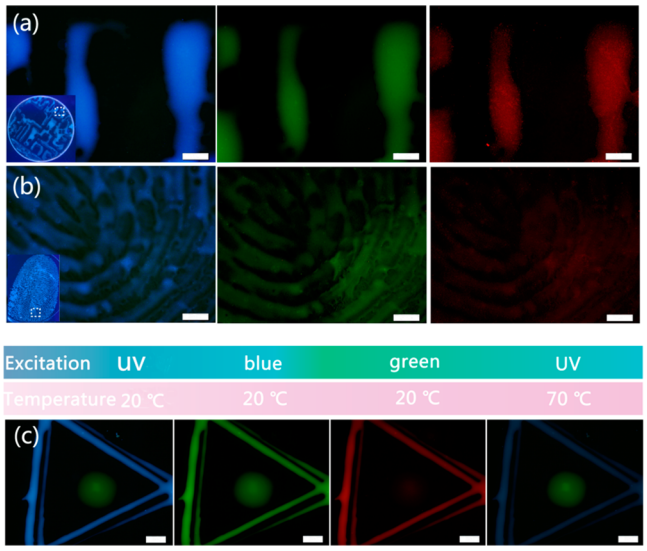

Figure 7. (a, b) Fluorescence microscope images of the selected zone of the stamp and fingerprint by using fluorescent silica nanodots ink under UV (left), blue (middle) and green light (right) excitation. (c) Fluorescent microscope images of pattern composed from silicon nanodots solutions (triangle) and commercially available green fluorescent ink (circle) under designated excitation light and temperature. Inset to a, b: Macroscopic photographs of stamp and fingerprint taken by a digital camera under UV lamp. The scale bar is 100 μm.

finding indicated that the silica nanodots-based fluorescent ink could be used as a novel material for anticounterfeiting technology with multiemission features that were difficult for counterfeiters to replicate. Furthermore, the water-soluble silica nanodots-based fluorescent ink could replace traditional inks to safely form clear, adelomorphic multifluorescent fingerprints and would no longer contaminate fingers (Figure 7b). Moreover, the printed characters and fingerprints retained their stability after one month in an indoor environment, which is beneficial for practical applications.

We further extended our study by combining the thermosensitive fluorescence and excitation-dependent emission together for a multifunctional pattern. As shown in Figure 7c, the pattern consisted of a triangle made from silicon nanodot and circle with commercially available green fluorescent ink. Under UV light excitation and room temperature, a fluorescent pattern with blue triangle and green circle was observed. In contrast, the dual-colored pattern changed to a single one upon the blue-light excitation. Only a red triangle could be observed while the excitation light changed from blue to green. When the temperature of the pattern increased (70 °C), the PL intensity of the triangle under UV illumination decreased significantly. Finally, pattern with highly luminescent blue triangle and green circle was again observed as the sample was cooled to room temperature. These results suggested the great potential of the as-prepared silica nanodots to be acted like chameleons that could respond to changes in their surroundings and adjust their skin color for an improved anticounterfeiting technology. Furthermore, the fluorescent pattern is expected to be easily changed to a different one for the anticounterfeiting technology by combination of materials of other optical properties with the prepared silica nanodots.

4. CONCLUSIONS

In conclusion, we have demonstrated an easy IL-assisted solution route to prepare water-soluble silica nanodots with good photostability, excitation-wavelength-dependent luminescence, and temperature sensitivity with both their fluorescence intensity and lifetime. This one-pot approach does not require specific equipment as well as harsh conditions. The ILs used in the present study not only provided the environment for the reaction but also contributed to the bright photoluminescence of the silica nanodots. We further extended the use of this highly luminescent nanomaterial for anticounterfeiting application and the results demonstrated the great potential of the silica nanodots alone or combined with fluorescent material of unicolor for an improved anticounterfeiting technology. This simple approach and the resulting outstanding combination of properties make the prepared silica nanodots highly promising for myriad applications in areas such as fluorescent anticounterfeiting, optoelectronic devices, medical diagnosis, and biological imaging.

■ ASSOCIATED CONTENT

Supporting Information

XPS spectra and UV−vis spectra of silica nanodots, PL spectra of silica nanodots prepared at different temperature and with increasing reaction time, PL spectra of the silica nanodots prepared in the presence of HCl and sodium dihydrogen phosphate, photographs of silica nanodots prepared with CDP, sodium dihydrogen phosphate and choline chloride, photographs of fresh silica gel and gel after two months of storage, photograph of dried silica gel, luminescence decay curve of silica nanodot, temperature-dependence of the PL of the silica nanodots solution, reversible temperature-dependence of the PL of the silica nanodots film, schematic representation of using fluorescent silica nanodots ink for stamps and fingerprints, and QY of silica nanodots prepared under different reaction conditions. This material is available free of charge via the Internet at http://pubs.acs.org.

DOI: 10.1021/am5083304
ACS Appl. Mater. Interfaces 2015, 7, 2905−2911

AUTHOR INFORMATION

Corresponding Authors

*E-mail: jren@ciac.ac.cn.

*E-mail: xqu@ciac.ac.cn.

Notes

The authors declare no competing financial interest.

ACKNOWLEDGMENTS

This work was supported by the National Basic Research Program of China (Grants 2012CB720602, 2011CB936004) and the National Natural Science Foundation of China (Grants 91213302, 21210002, 21431007, 91413111).

REFERENCES

(1) Peng, F.; Su, Y.; Zhong, Y.; Fan, C.; Lee, S.-T.; He, Y. Silicon Nanomaterials Platform for Bioimaging, Biosensing, and Cancer Therapy. *Acc. Chem. Res.* **2014**, *47*, 612−623.

(2) Cheng, X.; Lowe, S. B.; Reece, P. J.; Gooding, J. J. Colloidal Silicon Quantum Dots: from Preparation to the Modification of Self-assembled Monolayers (SAMs) for Bio-applications. *Chem. Soc. Rev.* **2014**, *43*, 2680−2700.

(3) Tang, L.; Cheng, J. Nonporous Silica Nanoparticles for Nanomedicine Application. *Nano Today* **2013**, *8*, 290−312.

(4) Green, W. H.; Le, K. P.; Grey, J.; Au, T. T.; Sailor, M. J. White Phosphors from a Silicate-Carboxylate Sol-Gel Precursor That Lack Metal Activator Ions. *Science* **1997**, *276*, 1826−1828.

(5) Jakob, A. M.; Schmedake, T. A. A Novel Approach to Monodisperse, Luminescent Silica Spheres. *Chem. Mater.* **2006**, *18*, 3173−3175.

(6) Bekiari, V.; Lianos, P. Tunable Photoluminescence from a Material Made by the Interaction between (3-Aminopropyl)-triethoxysilane and Organic Acids. *Chem. Mater.* **1998**, *10*, 3777−3779.

(7) Lin, J.; Yu, M.; Lin, C.; Liu, X. Multiform Oxide Optical Materials via the Versatile Pechini-Type Sol-Gel Process: Synthesis and Characteristics. *J. Phys. Chem. C* **2007**, *111*, 5835−5845.

(8) Davies, G.-L.; McCarthy, J. E.; Rakovich, A.; Gun'ko, Y. K. Towards White Luminophores: Developing Luminescent Silica on the Nanoscale. *J. Mater. Chem.* **2012**, *22*, 7358−7365.

(9) Engström, K.; Johnston, E. V.; Verho, O.; Gustafson, K. P. J.; Shakeri, M.; Tai, C.-W.; Bäckvall, J.-E. Co-immobilization of an Enzyme and a Metal into the Compartments of Mesoporous Silica for Cooperative Tandem Catalysis: An Artificial Metalloenzyme. *Angew. Chem., Int. Ed.* **2013**, *52*, 14006−14010.

(10) Gu, L.; Hall, D. J.; Qin, Z.; Anglin, E.; Joo, J.; Mooney, D. J.; Howell, S. B.; Sailor, M. J. In Vivo Time-Gated Fluorescence Imaging with Biodegradable Luminescent Porous Silicon Nanoparticles. *Nat. Commun.* **2013**, *4*, 2326.

(11) Chen, M. Y.; Klunk, M. D.; Diep, V. M.; Sailor, M. J. Electric-Field-Assisted Protein Transport, Capture, and Interferometric Sensing in Carbonized Porous Silicon Films. *Adv. Mater.* **2011**, *23*, 4537−4542.

(12) Chen, C.; Geng, J.; Pu, F.; Yang, X.; Ren, J.; Qu, X. Polyvalent Nucleic Acid/Mesoporous Silica Nanoparticle Conjugates: Dual Stimuli-Responsive Vehicles for Intracellular Drug Delivery. *Angew. Chem., Int. Ed.* **2011**, *50*, 882−886.

(13) Yang, X.; Liu, X.; Liu, Z.; Pu, F.; Ren, J.; Qu, X. Near-Infrared Light-Triggered, Targeted Drug Delivery to Cancer Cells by Aptamer Gated Nanovehicles. *Adv. Mater.* **2012**, *24*, 2890−2895.

(14) Kovalev, D.; Fujii, M. Silicon Nanocrystals: Photosensitizers for Oxygen Molecules. *Adv. Mater.* **2005**, *17*, 2531−2544.

(15) Warner, J. H.; Hoshino, A.; Yamamoto, K.; Tilley, R. D. Water-Soluble Photoluminescent Silicon Quantum Dots. *Angew. Chem., Int. Ed.* **2005**, *44*, 4550−4554.

(16) Kang, Z.; Tsang, C. H. A.; Zhang, Z.; Zhang, M.; Wong, N.-b.; Zapien, J. A.; Shan, Y.; Lee, S.-T. A Polyoxometalate-Assisted Electrochemical Method for Silicon Nanostructures Preparation: From Quantum Dots to Nanowires. *J. Am. Chem. Soc.* **2007**, *129*, 5326−5327.

(17) Kang, Z.; Tsang, C. H. A.; Wong, N.-B.; Zhang, Z.; Lee, S.-T. Silicon Quantum Dots: A General Photocatalyst for Reduction, Decomposition, and Selective Oxidation Reactions. *J. Am. Chem. Soc.* **2007**, *129*, 12090−12091.

(18) Zou, J.; Baldwin, R. K.; Pettigrew, K. A.; Kauzlarich, S. M. Solution Synthesis of Ultrastable Luminescent Siloxane-Coated Silicon Nanoparticles. *Nano Lett.* **2004**, *4*, 1181−1186.

(19) Neiner, D.; Chiu, H. W.; Kauzlarich, S. M. Low-Temperature Solution Route to Macroscopic Amounts of Hydrogen Terminated Silicon Nanoparticles. *J. Am. Chem. Soc.* **2006**, *128*, 11016−11017.

(20) Holmes, J. D.; Ziegler, K. J.; Doty, R. C.; Pell, L. E.; Johnston, K. P.; Korgel, B. A. Highly Luminescent Silicon Nanocrystals with Discrete Optical Transitions. *J. Am. Chem. Soc.* **2001**, *123*, 3743−3748.

(21) Shirahata, N.; Hasegawa, T.; Sakka, Y.; Tsuruoka, T. Size-Tunable UV-Luminescent Silicon Nanocrystals. *Small* **2010**, *6*, 915−921.

(22) Henderson, E. J.; Shuhendler, A. J.; Prasad, P.; Baumann, V.; Maier-Flaig, F.; Faulkner, D. O.; Lemmer, U.; Wu, X. Y.; Ozin, G. A. Colloidally Stable Silicon Nanocrystals with Near-Infrared Photoluminescence for Biological Fluorescence Imaging. *Small* **2011**, *7*, 2507−2516.

(23) Das, P.; Saha, A.; Maity, A. R.; Ray, S. C.; Jana, N. R. Silicon Nanoparticle Based Fluorescent Biological Label via Low Temperature Thermal Degradation of Chloroalkylsilane. *Nanoscale* **2013**, *5*, 5732−5737.

(24) Shiohara, A.; Hanada, S.; Prabakar, S.; Fujioka, K.; Lim, T. H.; Yamamoto, K.; Northcote, P. T.; Tilley, R. D. Chemical Reactions on Surface Molecules Attached to Silicon Quantum Dots. *J. Am. Chem. Soc.* **2009**, *132*, 248−253.

(25) Li, Q.; He, Y.; Chang, J.; Wang, L.; Chen, H.; Tan, Y.-W.; Wang, H.; Shao, Z. Surface-Modified Silicon Nanoparticles with Ultrabright Photoluminescence and Single-Exponential Decay for Nanoscale Fluorescence Lifetime Imaging of Temperature. *J. Am. Chem. Soc.* **2013**, *135*, 14924−14927.

(26) Rosso-Vasic, M.; Spruijt, E.; van Lagen, B.; De Cola, L.; Zuilhof, H. Alkyl-Functionalized Oxide-Free Silicon Nanoparticles: Synthesis and Optical Properties. *Small* **2008**, *4*, 1835−1841.

(27) Erogbogbo, F.; Yong, K.-T.; Roy, I.; Xu, G.; Prasad, P. N.; Swihart, M. T. Biocompatible Luminescent Silicon Quantum Dots for Imaging of Cancer Cells. *ACS Nano* **2008**, *2*, 873−878.

(28) Hessel, C. M.; Rasch, M. R.; Hueso, J. L.; Goodfellow, B. W.; Akhavan, V. A.; Puvanakrishnan, P.; Tunnel, J. W.; Korgel, B. A. Alkyl Passivation and Amphiphilic Polymer Coating of Silicon Nanocrystals for Diagnostic Imaging. *Small* **2010**, *6*, 2026−2034.

(29) Zhong, Y.; Peng, F.; Bao, F.; Wang, S.; Ji, X.; Yang, L.; Su, Y.; Lee, S.-T.; He, Y. Large-Scale Aqueous Synthesis of Fluorescent and Biocompatible Silicon Nanoparticles and Their Use as Highly Photostable Biological Probes. *J. Am. Chem. Soc.* **2013**, *135*, 8350−8356.

(30) Zhang, J.; Yu, S.-H. Highly Photoluminescent Silicon Nanocrystals for Rapid, Label-Free and Recyclable Detection of Mercuric Ions. *Nanoscale* **2014**, *6*, 4096−4101.

(31) Zhong, Y.; Peng, F.; Wei, X.; Zhou, Y.; Wang, J.; Jiang, X.; Su, Y.; Su, S.; Lee, S.-T.; He, Y. Microwave-Assisted Synthesis of Biofunctional and Fluorescent Silicon Nanoparticles Using Proteins as Hydrophilic Ligands. *Angew. Chem., Int. Ed.* **2012**, *51*, 8485−8489.

(32) Wang, J.; Sun, S.; Peng, F.; Cao, L.; Sun, L. Efficient One-Pot Synthesis of Highly Photoluminescent Alkyl-Functionalised Silicon Nanocrystals. *Chem. Commun.* **2011**, *47*, 4941−4943.

(33) Lin, P.-Y.; Hsieh, C.-W.; Kung, M.-L.; Hsieh, S. Substrate-Free Self-Assembled SiO_x-Core Nanodots from Alkylalkoxysilane as a Multicolor Photoluminescence Source for Intravital Imaging. *Sci. Rep.* **2013**, *3*, 1703.

(34) Welton, T. Room-Temperature Ionic Liquids. Solvents for Synthesis and Catalysis. *Chem. Rev.* **1999**, *99*, 2071−2084.

(35) Plechkova, N. V.; Seddon, K. R. Applications of Ionic Liquids in the Chemical Industry. *Chem. Soc. Rev.* **2008**, *37*, 123−150.

DOI: 10.1021/am5083304
ACS Appl. Mater. Interfaces 2015, 7, 2905−2911

(36) Lin, Y.; Zhao, A.; Tao, Y.; Ren, J.; Qu, X. Ionic Liquid as an Efficient Modulator on Artificial Enzyme System: Toward the Realization of High-Temperature Catalytic Reactions. *J. Am. Chem. Soc.* **2013**, *135*, 4207−4210.
(37) Xing, H.; Liao, C.; Yang, Q.; Veith, G. M.; Guo, B.; Sun, X.-G.; Ren, Q.; Hu, Y.-S.; Dai, S. Ambient Lithium−SO_2 Batteries with Ionic Liquids as Electrolytes. *Angew. Chem., Int. Ed.* **2014**, *53*, 2099−2103.
(38) Vijayaraghavan, R.; Izgorodin, A.; Ganesh, V.; Surianarayanan, M.; MacFarlane, D. R. Long-Term Structural and Chemical Stability of DNA in Hydrated Ionic Liquids. *Angew. Chem., Int. Ed.* **2010**, *49*, 1631−1633.
(39) Ma, Z.; Yu, J.; Dai, S. Preparation of Inorganic Materials Using Ionic Liquids. *Adv. Mater.* **2010**, *22*, 261−285.
(40) Zhang, P.; Wu, T.; Han, B. Preparation of Catalytic Materials Using Ionic Liquids as the Media and Functional Components. *Adv. Mater.* **2014**, *26*, 6810−6827.
(41) Campbell, P. S.; Lorbeer, C.; Cybinska, J.; Mudring, A.-V. One-Pot Synthesis of Luminescent Polymer-Nanoparticle Composites from Task-Specific Ionic Liquids. *Adv. Funct. Mater.* **2013**, *23*, 2924−2931.
(42) Zhu, Y.-J.; Wang, W.-W.; Qi, R.-J.; Hu, X.-L. Microwave-Assisted Synthesis of Single-Crystalline Tellurium Nanorods and Nanowires in Ionic Liquids. *Angew. Chem., Int. Ed.* **2004**, *43*, 1410−1414.
(43) Zhou, Y.; Antonietti, M. A Series of Highly Ordered, Super-Microporous, Lamellar Silicas Prepared by Nanocasting with Ionic Liquids. *Chem. Mater.* **2003**, *16*, 544−550.
(44) Zhao, Y.; Zhang, J.; Han, B.; Song, J.; Li, J.; Wang, Q. Metal-Organic Framework Nanospheres with Well-Ordered Mesopores Synthesized in an Ionic Liquid/CO_2/Surfactant System. *Angew. Chem., Int. Ed.* **2011**, *50*, 636−639.
(45) Hoang, P. H.; Park, H.; Kim, D.-P. Ultrafast and Continuous Synthesis of Unaccommodating Inorganic Nanomaterials in Droplet- and Ionic Liquid-Assisted Microfluidic System. *J. Am. Chem. Soc.* **2011**, *133*, 14765−14770.
(46) Li, J.-R.; Xie, Z.-L.; He, X.-W.; Li, L.-H.; Huang, X.-Y. Crystalline Open-Framework Selenidostannates Synthesized in Ionic Liquids. *Angew. Chem., Int. Ed.* **2011**, *50*, 11395−11399.
(47) Zhao, X.; Jin, W.; Cai, J.; Ye, J.; Li, Z.; Ma, Y.; Xie, J.; Qi, L. Shape- and Size-Controlled Synthesis of Uniform Anatase TiO_2 Nanocuboids Enclosed by Active {100} and {001} Facets. *Adv. Funct. Mater.* **2011**, *21*, 3554−3563.
(48) Choi, B. G.; Yang, M.; Jung, S. C.; Lee, K. G.; Kim, J.-G.; Park, H.; Park, T. J.; Lee, S. B.; Han, Y.-K.; Huh, Y. S. Enhanced Pseudocapacitance of Ionic Liquid/Cobalt Hydroxide Nanohybrids. *ACS Nano* **2013**, *7*, 2453−2460.
(49) Jacob, D. S.; Joseph, A.; Mallenahalli, S. P.; Shanmugam, S.; Makhluf, S.; Calderon-Moreno, J.; Koltypin, Y.; Gedanken, A. Rapid Synthesis in Ionic Liquids of Room-Temperature-Conducting Solid Microsilica Spheres. *Angew. Chem., Int. Ed.* **2005**, *44*, 6560−6563.
(50) Liu, D.-P.; Li, G.-D.; Su, Y.; Chen, J.-S. Highly Luminescent ZnO Nanocrystals Stabilized by Ionic-Liquid Components. *Angew. Chem., Int. Ed.* **2006**, *45*, 7370−7373.
(51) Ding, K.; Miao, Z.; Liu, Z.; Zhang, Z.; Han, B.; An, G.; Miao, S.; Xie, Y. Facile Synthesis of High Quality TiO_2 Nanocrystals in Ionic Liquid via a Microwave-Assisted Process. *J. Am. Chem. Soc.* **2007**, *129*, 6362−6363.
(52) Lian, J.; Duan, X.; Ma, J.; Peng, P.; Kim, T.; Zheng, W. Hematite (α-Fe_2O_3) with Various Morphologies: Ionic Liquid-Assisted Synthesis, Formation Mechanism, and Properties. *ACS Nano* **2009**, *3*, 3749−3761.
(53) Vijayaraghavan, R.; Thompson, B. C.; MacFarlane, D. R.; Kumar, R.; Surianarayanan, M.; Aishwarya, S.; Sehgal, P. K. Biocompatibility of Choline Salts as Crosslinking Agents for Collagen Based Biomaterials. *Chem. Commun.* **2010**, *46*, 294−296.
(54) Prime, E. L.; Solomon, D. H. Australia's Plastic Banknotes: Fighting Counterfeit Currency. *Angew. Chem., Int. Ed.* **2010**, *49*, 3726−3736.
(55) Liu, Y.; Ma, X.; Lin, Z.; He, M.; Han, G.; Yang, C.; Xing, Z.; Zhang, S.; Zhang, X. Imaging Mass Spectrometry with a Low-Temperature Plasma Probe for the Analysis of Works of Art. *Angew. Chem., Int. Ed.* **2010**, *49*, 4435−4437.
(56) Widjaja, E.; Garland, M. Use of Raman Microscopy and Band-Target Entropy Minimization Analysis To Identify Dyes in a Commercial Stamp. Implications for Authentication and Counterfeit Detection. *Anal. Chem.* **2008**, *80*, 729−733.
(57) Qu, S.; Wang, X.; Lu, Q.; Liu, X.; Wang, L. A Biocompatible Fluorescent Ink Based on Water-Soluble Luminescent Carbon Nanodots. *Angew. Chem., Int. Ed.* **2012**, *51*, 12215−12218.
(58) Wang, J.; Wei, T.; Li, X.; Zhang, B.; Wang, J.; Huang, C.; Yuan, Q. Near-Infrared-Light-Mediated Imaging of Latent Fingerprints based on Molecular Recognition. *Angew. Chem., Int. Ed.* **2014**, *53*, 1616−1620.
(59) Zhao, J.; Jin, D.; Schartner, E. P.; Lu, Y.; Liu, Y.; Zvyagin, A. V.; Zhang, L.; Dawes, J. M.; Xi, P.; Piper, J. A.; Goldys, E. M.; Monro, T. M. Single-Nanocrystal Sensitivity Achieved by Enhanced Upconversion Luminescence. *Nat. Nanotechnol.* **2013**, *8*, 729−734.
(60) Liu, Y.; Ai, K.; Lu, L. Designing Lanthanide-Doped Nanocrystals with Both Up- and Down-Conversion Luminescence for Anti-counterfeiting. *Nanoscale* **2011**, *3*, 4804−4810.
(61) Andres, J.; Hersch, R. D.; Moser, J.-E.; Chauvin, A.-S. A New Anti-Counterfeiting Feature Relying on Invisible Luminescent Full Color Images Printed with Lanthanide-Based Inks. *Adv. Funct. Mater.* **2014**, *24*, 5029−5036.

DOI: 10.1021/am5083304
ACS Appl. Mater. Interfaces 2015, 7, 2905−2911